

# Synthesis and structural study of quinoline( $\mu$ 1, $\mu$ 3)-thiocyanate silver(I) complex

Anastasia Gayatri Marwan<sup>1</sup>, Putri Dwi Lestari<sup>1</sup>, M. Robitul Choir<sup>1</sup>, Sutandyo Dwija Laksmna<sup>1</sup>, Adilah Aliyatulmuna<sup>1</sup>, and I Wayan Dasna<sup>1\*</sup>

<sup>1</sup>Departemen Kimia, FMIPA, Universitas Negeri Malang, Jalan Semarang 5, Malang, Indonesia 65145

**Abstract.** A new quinoline( $\mu$ 1, $\mu$ 3)-thiocyanatesilver(I) complex,  $[\text{Ag}(\text{Q})(\text{SCN})]_n$ , (Q = quinoline,  $\text{C}_9\text{H}_7\text{N}$ ) has been successfully synthesized through a direct reaction at room temperature between silver(I) nitrate, quinoline ligand, and potassium thiocyanate in a 1:1:1 molar ratio. Colorless crystals were obtained after nine days of evaporation. FT-IR analysis confirmed the presence of characteristic functional groups from both quinoline and  $\text{SCN}^-$  ligands. Refinement results from SC-XRD indicated that the silver(I) complex crystallizes in a pseudo-tetrahedral structure with an orthorhombic crystal system and space group P 212121 ( $a = 4.0877(2)$  Å,  $b = 13.4948(8)$  Å,  $c = 18.0710(11)$  Å;  $\alpha = \beta = \gamma = 90^\circ$ ). The R-factor value of 6.78% demonstrates that the refined structure is in close agreement with the actual molecular arrangement. Hirshfeld surface analysis further revealed intermolecular interactions with distances shorter than 8 Å, in which the dominant contact is  $\text{H}\cdots\text{H}$ , contributing 29.2% of the total interactions. Antibacterial testing against *Staphylococcus aureus* and *Escherichia coli* revealed moderate activity, higher than the free ligands but lower than  $\text{AgNO}_3$  and chloramphenicol, indicating that Ag(I) coordination enhances antibacterial performance.

## 1 Introduction

The synthesis of antibacterial compounds represents a new approach to overcoming the resistance of pathogenic bacteria to conventional antibiotics, with the aim of enhancing effectiveness against resistant bacterial strains [1]. Coordination-based antibacterial compounds, formed through interactions between metal ions and ligands, can enhance stability, bioavailability, and biological activity against bacteria. Metal ions such as  $\text{Cu}^{2+}$ ,  $\text{Ag}^+$ , and  $\text{Mn}^{2+}$  are commonly reacted with organic ligands using appropriate solvents. The ligands employed may consist of a combination of two different types to optimize their antibacterial properties [2].

Among various antibacterial metals, silver(I) is particularly attractive due to its versatile coordination chemistry and well-documented antimicrobial properties. Metal complexes can work independently or be combined with antibiotics through the mechanism of Reactive Oxygen Species (ROS) production, which damages bacterial DNA, membranes, and proteins, as well as interfering with the metabolism of metal ions. Gram-positive bacteria are more susceptible

\*Corresponding author: [idasna@um.ac.id](mailto:idasna@um.ac.id)

because they have thicker cell walls, making lipophilic molecules more able to penetrate more easily. These metal complexes can act independently or in combination with antibiotics through the mechanism of Reactive Oxygen Species (ROS) production, which damages bacterial DNA, membranes, and proteins, and inhibits key enzymes involved in metal ion metabolism. Gram-positive bacteria are generally more susceptible due to their thick cell wall lacking an outer membrane, allowing lipophilic molecules to penetrate more easily [2].

Silver(I) is among the most frequently utilized metal ions in coordination chemistry because it can adopt diverse geometries and coordination modes. Complexes of silver(I) with pyridine and its derivatives have attracted considerable interest, as their structural flexibility enables the formation of polymers, dimers, and polynuclear frameworks that exhibit notable biological activity and good thermal stability. Silver salts tend to dissolve more readily in water, which leads to a faster release of  $\text{Ag}^+$  ions compared to silver complexes. This allows free  $\text{Ag}^+$  ions to diffuse more efficiently and interact with active sites on bacterial proteins or cellular components. Silver(I) complexes containing bidentate ligands such as  $\text{WO}_4^{2-}$ ,  $[\text{N}(\text{CN})_2]^-$ ,  $\text{SCN}^-$ , and  $\text{NCO}^-$  are also known to form polymeric structures in one-, two-, or three-dimensional arrangements. Consequently, Ag(I) complexes employing bridging ligands warrant further investigation to better understand their structural properties and explore their potential applications [3].

The choice of quinoline-based ligands is motivated by their well-established biological activities, as they have been widely employed in anti-HIV and antimalarial therapies and as pharmacological antagonists against neurotoxins. Quinoline is also known for its pronounced toxicity toward aquatic bacteria and fish, which is influenced by the length of its alkyl chain and the nature of its substituents. Another advantage of quinoline ligands lies in their structural characteristics. The presence of  $\pi$ - $\pi$  stacking interactions an essential form of interaction between molecules containing conjugated aromatic systems (such as quinoline) can significantly influence the overall structural arrangement of Ag(I) complexes [4].

The antibacterial activity of Ag-quinoline complexes primarily arises from  $\text{Ag}^+$  ions, which damage bacterial proteins, membranes, and DNA through the generation of reactive oxygen species (ROS). Coordination with the quinoline ligand stabilizes and controls the release of  $\text{Ag}^+$ , while the aromatic and lipophilic nature of quinoline enhances membrane penetration. Substituent variations on the quinoline ring further influence the effectiveness of the complexes, with certain derivatives exhibiting larger inhibition zones than the free ligands or silver salts. Overall, Ag-quinoline complexes demonstrate strong antibacterial activity with dual mechanisms and high structural stability [4].

Hirshfeld Surface Analysis is employed to complement characterization methods by visualizing intermolecular interactions within the crystal structure in three dimensions, such as hydrogen bonding and  $\pi$ - $\pi$  interactions. The red regions on the Hirshfeld map indicate short contacts (stronger interactions, closer than Van der Waals distance), while blue regions represent long contacts (weaker interactions). This analysis provides a deeper understanding of the interactions that contribute to the stability of the crystal structure [5].

The objective of this study is to synthesize and characterize a new  $[\text{Ag}(\text{Q})(\text{SCN})]_n$  complex and to evaluate its antibacterial activity against both Gram-positive (*Staphylococcus aureus*) and Gram-negative (*Escherichia coli*) bacteria. This research aims to elucidate the relationship between the coordination structure of the complex and its antibacterial effectiveness, as well as to assess its potential as a metal-based antimicrobial agent with a controlled mechanism of action through the stabilized release of  $\text{Ag}^+$  ions. The evaluation is also expected to provide insights into the ability of the complex to inhibit bacteria with different cell wall characteristics.

## 2 Experimental

### 2.1 Materials

AgNO<sub>3</sub> Merck, p.a, quinoline Merck, p.a, dan KSCN Merck, p.a, Amonia, Asetonitril, Aquades

### 2.2 Procedure

#### 2.2.2 Synthesis of the [Ag(Q)(SCN)]<sub>n</sub> Complex

The synthesis of the [Ag(Q)(SCN)]<sub>n</sub> complex involves dissolving 1 mmol of quinoline in 5 mL of acetonitrile. Then, dissolve 1 mmol of AgNO<sub>3</sub> in 5 mL of water and 1 mmol of KSCN in 5 mL of water. Mix the AgNO<sub>3</sub> and KSCN solutions. Afterward, collect the precipitate and dissolve it in ammonia 98% and the quinoline solution. Then, cover the container with aluminum foil and stir the solution for 24 hours in a dark condition. Finally, allow the solution to evaporate slowly under dark conditions at room temperature until crystals are formed.

#### 2.2.3 Characterization Techniques

The characterization of the complex compound was carried out using several methods, including the determination of melting point, electrical conductivity measurements, FT-IR analysis, and single crystal XRD analysis. The melting point was determined using a Fisher-Johns Melting Point Apparatus in the temperature range of 28–350°C with a heating rate of 20°C/min. Electrical conductivity was measured using a Cyberscan CON 11/110 conductivity meter in methanol solution at room temperature. The FT-IR spectrum was obtained using a Shimadzu IR Prestige-21 spectrometer in the wave number range of 500–4000 cm<sup>-1</sup>. Meanwhile, the crystal structure analysis was performed using a Bruker D8 Quest single crystal X-ray diffractometer.

#### 2.2.4 Antibacterial Activity Test

The antibacterial activity test of the complex compound was conducted at the Integrated Laboratory of Universitas Negeri Malang, Indonesia, using the agar diffusion method (Kirby–Bauer). The test was performed against *Escherichia coli* (ATCC 25922) and *Staphylococcus aureus* (ATCC 25923), with chloramphenicol used as a positive control. In this procedure, 10 mL of nutrient agar was poured into each Petri dish, followed by the addition of 100 µL of bacterial suspension. The complex compound was dissolved in 10% dimethyl sulfoxide (DMSO) until the final concentration reached 5 mg/mL. Subsequently, the solution was applied to sterile paper discs, which were then placed on the agar surface. The Petri dishes were incubated at 37 °C for 24 hours, and after incubation, the diameter of the bacterial growth inhibition zones was measured.

#### 2.2.5 Hirshfeld Surface Analysis

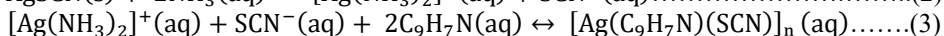
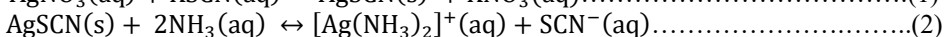
Hirshfeld surface analysis was performed using CrystalExplorer software. The purpose of this analysis is to visualize intermolecular interactions on the crystal surface, which helps in understanding the packing pattern of the crystal. The strength of intermolecular interactions was determined through the three-dimensional dnorm surface, visualized in a fixed color scale, ranging from 0.0870 (red) to 1.2944 (blue). Additionally, a fingerprint plot was displayed in the

distance range of 1.0–2.8 Å, projected along the graph axis to illustrate the distribution of these interactions.

### 3 Results and Discussion

#### 3.1 Synthesis of the Complex

The new complex  $[\text{Ag}(\text{Q})(\text{SCN})]_n$  was successfully synthesized through the reaction of  $\text{AgNO}_3$  with quinoline and  $\text{KSCN}$  at a 1:1:1 molar ratio using a direct reaction method at room temperature for 24 hours. Crystals were obtained after aging for 9 days, with the crystals being needle-shaped and colorless.



Ammonia was added to the reaction system to dissolve the initially formed  $\text{AgSCN}$  precipitate through the formation of the soluble intermediate  $[\text{Ag}(\text{NH}_3)_2]^+$ , thereby preventing the loss of  $\text{Ag}^+$  species and ensuring their availability for subsequent coordination with the quinoline and thiocyanate ligands. The presence of ammonia also stabilizes  $\text{Ag}^+$  in solution and promotes a controlled complexation process, ultimately enabling the successful formation and crystallization of the desired  $[\text{Ag}(\text{C}_9\text{H}_7\text{N})(\text{SCN})]_n$  complex.

#### 2.3 Characterization

##### 2.3.1 Melting Point Determination

The melting point test is conducted to assess the decomposition and thermal stability of the ligands as well as the synthesized metal complexes. A sharp melting point indicates a pure compound, while a deviation in the melting point suggests the presence of impurities or incomplete complexation. In coordination chemistry, this data is also used to confirm the formation of a new, stable compound that is distinct from its reactants [6]. The complex product  $[\text{Ag}(\text{Q})(\text{SCN})]_n$  shows a thermal transition at 184 °C, differing from its precursor reactants, namely  $\text{AgNO}_3$  (212 °C), quinoline (-15 °C), and  $\text{KSCN}$  (173 °C). The difference in melting points indicates that the product is not a physical mixture but a new compound with thermal characteristics typical of coordination complexes. Therefore, the melting point data support the conclusion that a new compound has been formed from the  $\text{Ag}(\text{I})$ ,  $\text{SCN}$ , and quinoline complex, exhibiting thermal properties that differ from those of its reactants [7].

**Table 1.** Melting point data of the reactants and the synthesized complex  $[\text{Ag}(\text{Q})(\text{SCN})]_n$

Compound	Melting Point (°C)
$\text{AgNO}_3$	212
Quinoline	-15
$\text{KSCN}$	173
$[\text{Ag}(\text{Q})(\text{SCN})]_n$	184

### 2.3.2 FT-IR Analysis

FT-IR (Fourier Transform Infrared Spectroscopy) analysis is performed to identify functional groups and the coordination patterns of ligands towards metal atoms in the synthesized complexes. Shifts and changes in the intensity of absorption bands, especially in the C=O, C=N, and C–O regions, are used as indicators of bond formation between metal atoms and donor atoms such as nitrogen or oxygen. The FT-IR results provide strong spectral evidence to confirm the formation of new metal complexes and explain the changes in the electronic environment due to the coordination process [8].

The FT-IR spectrum of free quinoline shows a characteristic C–N stretching vibration at approximately  $1580\text{ cm}^{-1}$ , which shifts to a lower wavenumber ( $\approx 1550\text{ cm}^{-1}$ ) in the  $[\text{Ag}(\text{Q})(\text{SCN})]_n$  complex. This shift indicates the involvement of the quinoline nitrogen atom in coordination with the Ag(I) center. In contrast, the aromatic C=C stretching vibrations observed in the region of  $1450\text{--}1600\text{ cm}^{-1}$  remain nearly unchanged, suggesting that the aromatic ring system of quinoline is largely preserved after coordination. Importantly, the presence and coordination behavior of the thiocyanate ( $\text{SCN}^-$ ) ligand are evidenced by distinct vibrational bands. The strong band observed in the region of  $2100\text{--}2150\text{ cm}^{-1}$  corresponds to the  $\nu(\text{C}\equiv\text{N})$  stretching vibration of  $\text{SCN}^-$ , while the band appearing around  $700\text{--}800\text{ cm}^{-1}$  is attributed to the  $\nu(\text{C}\text{--}\text{S})$  stretching mode. These features confirm the incorporation of  $\text{SCN}^-$  into the coordination framework and support its role as a bridging ligand within the polymeric structure. Overall, the observed shifts in the C–N vibration of quinoline and the presence of characteristic  $\text{SCN}^-$  stretching bands provide spectroscopic evidence for successful coordination between Ag(I), quinoline, and thiocyanate, confirming the formation of the  $[\text{Ag}(\text{Q})(\text{SCN})]_n$  complex [9].

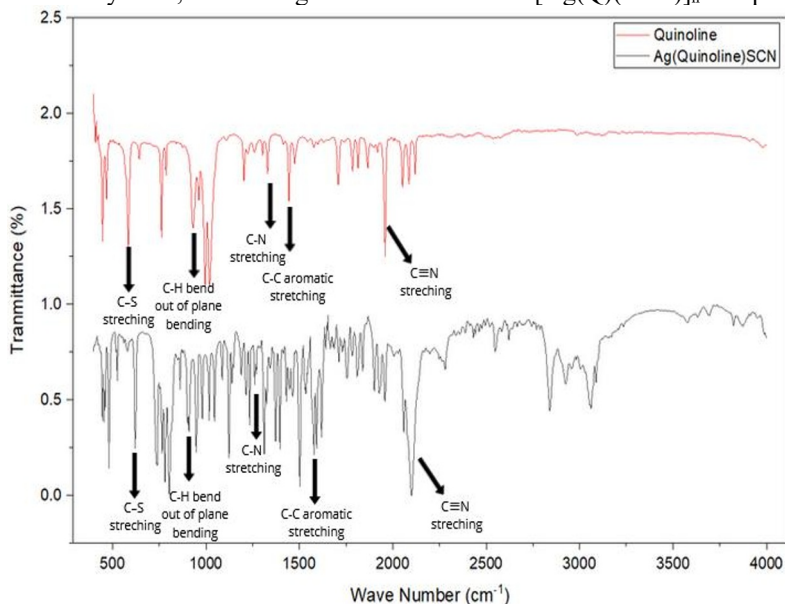


**Fig. 1.** FT-IR spectra of the complex  $[\text{Ag}(\text{Q})(\text{SCN})]_n$

### 2.3.3 Electrical Conductivity Test

The electrical conductivity test is conducted to determine the nature of the ionic bond and the type of coordination in the synthesized metal complexes. Conductivity values are used to assess whether the complexes are strong electrolytes, weak electrolytes, or non-electrolytes based on their ability to dissociate in solution. Low conductivity values indicate that the complexes possess

strong covalent bonds, with limited dissociation, and confirm the formation of stable metal complexes distinct from their free ligands [10].

The electrical conductivity measurement of the  $[\text{Ag}(\text{Q})(\text{SCN})]_n$  complex (0.1 M) yielded a value of 2.56 mS/cm, which is lower than that of  $\text{AgNO}_3$  (11.44 mS/cm) and  $\text{KSCN}$  (13.10 mS/cm). The difference indicates that the number of free ions is much lower in the complex, showing its behavior as a weak electrolyte or nearly a non-electrolyte compared to the free metal salts. This result supports the idea that the complexes formed involve stable covalent/coordination bonds and do not dissociate easily in solution [12]. This behavior is attributed to the highly coordinated nature of the  $\text{Ag}^+$  ion, which significantly restricts its dissociation. As a comparison, quinoline, which also forms a non-electrolyte, shows a much lower conductivity (4.66 mS/cm). This finding further confirms the relationship between ligand solubility and the ability to dissociate, which significantly impacts the electrical conductivity of the substance [4].

**Table 2.** Electrical conductivity of the solvent, reactant, and the complex  $[\text{Ag}(\text{Q})(\text{SCN})]_n$

Compound	Concentration	Electrical Conductivity (mS/cm)
$\text{AgNO}_3$	0.1 M	11.44
Quinoline	0.1 M	4.66
$\text{KSCN}$	0.1 M	13.10
$[\text{Ag}(\text{Q})(\text{SCN})]_n$	0.1 M	2.56

### 2.3.4 Single Crystal XRD Analysis

Single Crystal X-ray Diffraction (XRD) analysis is performed to determine the three-dimensional molecular structure and the coordination geometry of the complex. This technique provides accurate data on bond lengths, bond angles, and crystal space group, which helps confirm the formation of a new coordination complex that is different from its precursor [11]. Single crystal analysis of the  $[\text{Ag}(\text{Q})(\text{SCN})]_n$  complex shows that the compound crystallizes in an orthorhombic system with the space group  $\text{P}2_12_12_1$ .

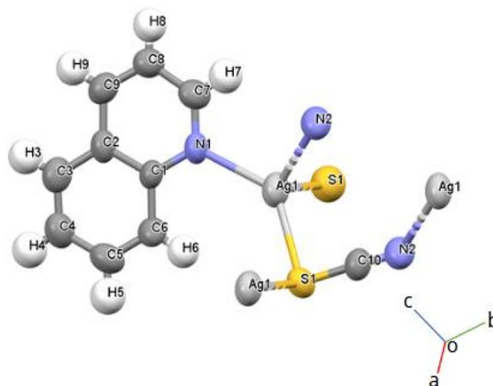


**Fig. 2.** Structure of the complex  $[\text{Ag}(\text{Q})(\text{SCN})]_n$

The bond length data shows that the central  $\text{Ag}(\text{I})$  in the  $[\text{Ag}(\text{Q})(\text{SCN})]_n$  complex is surrounded by an  $\text{N}_2\text{S}_2$  environment with a tetrahedral geometry. The  $\text{Ag}-\text{N}(\text{quinoline})$  bond is the shortest (2.28 Å), indicating a strong coordination with the nitrogen atom of the quinoline ring, while the  $\text{Ag}-\text{N}(\text{SCN})$  bond is slightly longer (2.33 Å), suggesting the role of  $\text{N}(\text{SCN})$  as a bridging ligand. The  $\text{Ag}-\text{S}$  bond length ranges between 2.53–2.68 Å, indicating a terminal bond and a weaker coordination compared to the  $\text{Ag}-\text{N}$  bonds. This variation confirms the formation of a stable coordination network that involves the interaction between  $\text{Ag}-\text{N}(\text{quinoline})$  and  $\text{Ag}-\text{S}/\text{N}(\text{SCN})$ .

**Table 3.** Crystallographic data of the complex  $[\text{Ag}(\text{Q})(\text{SCN})]_n$ 

Parameter	Value	
CCDC number	2487639	
Chemical formula	$\text{C}_{20} \text{H}_{14} \text{Ag}_2 \text{N}_4 \text{S}_2$	
Molecular weight	590.21	
Temperature	296.(2) K	
Wavelength	0.71073	
Crystal system	Orthorhombic	
Space group	P 2 <sub>1</sub> 2 <sub>1</sub> 2 <sub>1</sub>	
Lattice parameters	a 4.0877(2) b 13.4948(8) c 18.0710(11)	a 90 b 90 g 90
Volume	996.845	
Z	2	
Type of X-ray radiation	Mo K $\alpha$	
Crystal size (mm)	0.20	
Number of reflections for determination	10094	
F (ooo)	576	
R-Factor (%)	6.78	

**Table 4.** Bond lengths around the central Ag(I) atom of the complex  $[\text{Ag}(\text{Q})(\text{SCN})]_n$ 

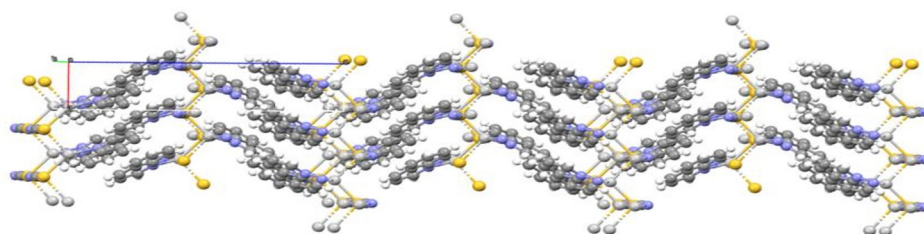
Bond	Bond Length (Å)
Ag1-S1	2.529(4)
Ag1-N1	2.28(1)
Ag1-S1'	2.677(4)
Ag1-N2	2.33(1)
S1'-Ag1	2.677(4)
N2'-Ag1	2.33(1)

The bond angle data shows that the central Ag(I) in the complex  $[\text{Ag}(\text{Q})(\text{SCN})]_n$  has an  $\text{N}_2\text{S}_2$  coordination with a distorted tetrahedral geometry. The main bond angle ranges from  $99^\circ$  to  $133^\circ$ , slightly deviating from the ideal value due to ligand effects. The Ag–N–C bond in the quinoline ring ( $124^\circ$ – $118^\circ$ ) indicates  $\text{sp}^2$  hybridization, while the C–N–Ag ( $\sim 140^\circ$ ) suggests coordination through the nearly linear N thiocyanate atom. Overall, the variation in bond angles and lengths emphasizes the formation of a 1D polymer chain stabilized by the strong coordination of Ag–N(quinoline) and the Ag–S/N(SCN) bridge.

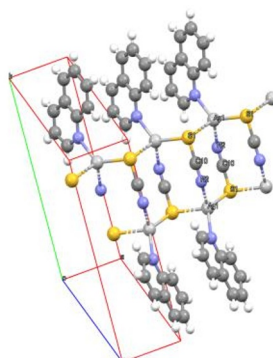
**Table 5.** Bond angle data around the central Ag(I) atom of the complex  $[\text{Ag}(\text{Q})(\text{SCN})]_n$ 

z	Angle ( $^\circ$ )
S1-Ag1-N1	132.7(3)
S1- Ag1-S1	103.4(1)
S1- Ag1-N2	108.5(3)
N1- Ag1-S1	106.3(3)
N1- Ag1-N2	99.2(4)
S1- Ag1-N2	103.7(3)
Ag1-S1-C10	96.6(5)
Ag1-S1- Ag1	103.4(1)
C10-S1- Ag1	96.5(5)
Ag1-N1-C1	124.6(8)
Ag1-N1- C1	117.9(9)
C10-N2- Ag1	140(1)

The structure of the  $[\text{Ag}(\text{Q})(\text{SCN})]_n$  complex forms a 1D chain arrangement along the crystal axis, creating a structure resembling a ladder. The coordination bond between Ag(I) and the quinoline ligand and  $\text{SCN}^-$  forms a stable structure, with hydrogen bonding playing a crucial role in crystal packing. The complex crystal packing is observed in a three-dimensional form, with the unit cell showing how the orientation and spatial dimensions form a crystal lattice. The complex molecules are closely packed through hydrogen interactions and  $\pi$ - $\pi$  stacking, which enhances the stability and packing of the crystal.



(a)



(b)

**Fig. 3.** a) Expanded complex structure, b) Crystal packing of the complex

### 2.3.5 Hirshfeld Surface Analysis

Hirshfeld Surface Analysis is performed to identify and measure the contribution of non-covalent interactions between molecules in the crystal structure. Through this analysis, the types and strengths of interactions, such as hydrogen bonding, van der Waals forces, and  $\pi$ - $\pi$  stacking, which play important roles in stability and crystal packing, can be identified. By visualizing the color maps on the molecular surface and analyzing the two-dimensional fingerprint plots, the method provides quantitative insights into how molecules interact with each other [12].

Hirshfeld Surface Analysis is performed to identify and visualize intermolecular contacts in the crystal structure, particularly non-covalent interactions such as  $\text{H}\cdots\text{H}$ ,  $\text{C}\cdots\text{H}$ , and  $\text{H}\cdots\text{Cl}/\text{Cl}\cdots\text{H}$ . The dnorm mapping represents interaction areas through a color gradient: red for short contacts (strong interactions), white for neutral distances, and blue for long contacts (weak interactions). This analysis provides visual and quantitative insights into the contribution of intermolecular interactions to the stability and crystal packing of metal complexes [13]. The red areas on the surface represent the Ag-S bond, indicating a significant interaction between silver (Ag) and sulfur (S). The surface shows areas where this interaction is stronger, marked with red or more pronounced regions.



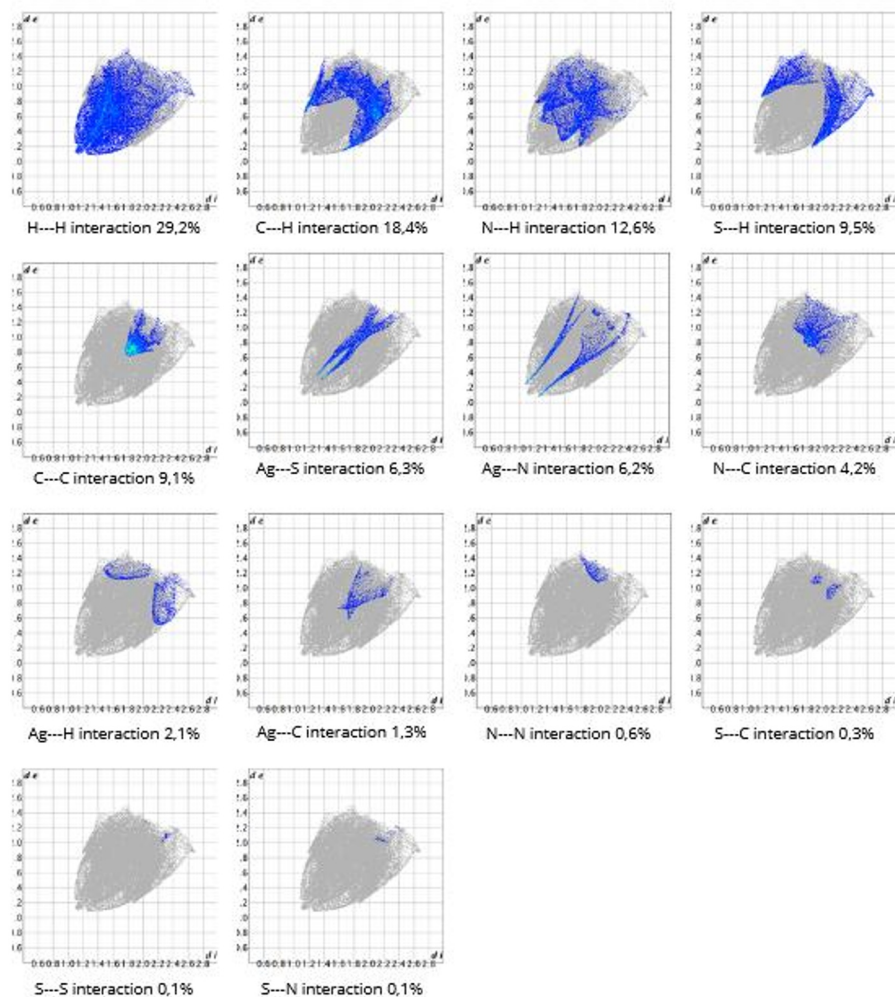


Fig. 5. Individual atom interactions in crystal packing  $[Ag(Q)(SCN)]_n$

### 2.3.6 Antibacterial Properties

The antibacterial activity of the  $[Ag(Q)(SCN)]_n$  complex was evaluated using the Kirby–Bauer disk diffusion method against *Staphylococcus aureus* (Gram-positive) and *Escherichia coli* (Gram-negative). As shown in Table 6, the complex exhibited inhibition zones of 11.22 mm against *S. aureus* and 11.15 mm against *E. coli*. These values are higher than those of the free quinoline ligand (8.00 and 7.00 mm) and KSCN (10.00 and 6.70 mm), but remain lower than those of  $AgNO_3$  (12.60 and 14.00 mm) and the standard antibiotic chloramphenicol (26.10 and 28.20 mm).

The observed increase in inhibition zones relative to the free ligand indicates that complex formation between  $Ag(I)$ , quinoline, and  $SCN^-$  contributes to the antibacterial activity. However, the underlying antibacterial mechanism cannot be conclusively determined from the present data. The involvement of metal–ligand coordination and changes in the physicochemical properties of the complex may influence the antibacterial response, but such interpretations should be treated with caution, as no statistical analysis or  $Ag^+$  release or stability studies were conducted [3].

Although the antibacterial activity of the  $[\text{Ag}(\text{Q})(\text{SCN})]_n$  complex is lower than that of  $\text{AgNO}_3$  and chloramphenicol, the results demonstrate that the complex exhibits moderate antibacterial activity. Therefore, this complex may be considered as an initial screening candidate for silver-based antibacterial agents. Further investigations, including statistical evaluation, stability assessment, and mechanistic studies, are required to clarify its antibacterial mechanism and practical applicability.

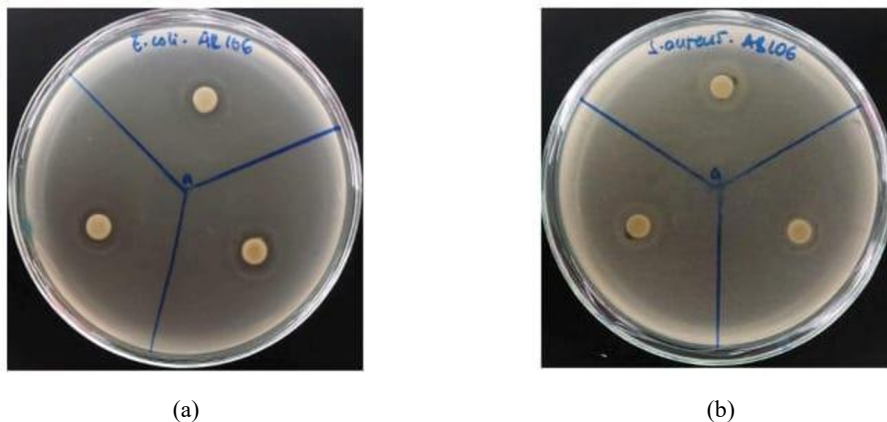


**Fig 6.** Inhibition zones of complex against (a) *S.aureus*, (b) *E.coli*

**Table 6.** Inhibition zones of compounds

No	Compounds	Inhibition zone (mm)	
		<i>S.aureus</i>	<i>E.coli</i>
1	$[\text{Ag}(\text{Q})(\text{SCN})]_n$	11,22	11,15
2	KSCN	10,00	6,70
3	Quinoline	8,00	7,00
4	$\text{AgNO}_3$	12,60	14,00
5	Chloramphenicol	26,10	28,20

## 4 Conclusion

The coordination polymer  $[\text{Ag}(\text{Q})(\text{SCN})]_n$  was successfully synthesized through a direct reaction between  $\text{AgNO}_3$ , quinoline, and KSCN in a 1:1:1 molar ratio at room temperature. Colorless needle-shaped crystals were obtained after nine days of slow evaporation, indicating the formation of a well-defined crystalline product. The melting point of the complex (184 °C), which differs from those of  $\text{AgNO}_3$ , quinoline, and KSCN, confirms the formation of a new compound with distinct thermal properties.

FT-IR analysis revealed a shift of the quinoline C–N stretching vibration from  $\sim 1580\text{ cm}^{-1}$  to  $\sim 1550\text{ cm}^{-1}$  upon coordination, indicating the involvement of the quinoline nitrogen atom in binding to the Ag(I) center. The presence of thiocyanate coordination was confirmed by characteristic  $\nu(\text{C}\equiv\text{N})$  and  $\nu(\text{C}-\text{S})$  stretching bands, supporting the role of  $\text{SCN}^-$  as a bridging ligand. Electrical conductivity measurements (2.56 mS/cm) indicate that the complex behaves as a weak electrolyte or near non-electrolyte, suggesting the formation of stable covalent/coordination bonds with limited dissociation in solution.

Single-crystal XRD analysis demonstrated that  $[\text{Ag}(\text{Q})(\text{SCN})]_n$  crystallizes in an orthorhombic crystal system with space group  $\text{P2}_12_12_1$ , featuring a distorted tetrahedral  $\text{N}_2\text{S}_2$  coordination environment around the Ag(I) center. The structure forms a one-dimensional polymeric chain through  $\mu_1, \mu_3$ -thiocyanate bridging, further stabilized by hydrogen bonding and  $\pi$ - $\pi$  stacking interactions between quinoline rings. Hirshfeld surface analysis confirmed that

H $\cdots$ H interactions dominate crystal packing (29.2%), followed by C $\cdots$ H, N $\cdots$ H, S $\cdots$ H, and  $\pi$ - $\pi$  stacking contributions, collectively enhancing structural stability.

Antibacterial evaluation against *Staphylococcus aureus* and *Escherichia coli* showed inhibition zones of 11.22 mm and 11.15 mm, respectively. These values are higher than those of the free ligands but lower than AgNO<sub>3</sub> and chloramphenicol, indicating moderate antibacterial activity. The enhanced activity relative to the ligands is attributed to Ag(I) coordination, which alters physicochemical properties and may facilitate controlled Ag<sup>+</sup> availability. Overall, [Ag(Q)(SCN)]<sub>n</sub> represents a structurally stable silver(I) coordination polymer with moderate antibacterial potential, warranting further investigation to clarify its antibacterial mechanism and practical applicability.

## Acknowledgments

The authors would like to express their sincere appreciation to the Direktorat Jenderal Pendidikan Tinggi, Riset dan Teknologi Kementerian Pendidikan, Kebudayaan, Riset dan Teknologi, Indonesia for providing financial support for this research through the fundamental research grant in 2025 (Contract No. 24.2.799/UN32.14.1/LT/2025). We would like to express our sincere gratitude to I Wayan Dasna, our supervisor and corresponding author, for his invaluable guidance, support, and insights throughout the development of this article. His expertise and constructive feedback were essential in shaping the direction of this work. We also extend our deepest thanks to Adilah Aliyatulmuna, Putri Dwi Lestari, M. Robitul Choir, and Sutandyo Dwija Laksana for their significant contributions to the creation of this article. Their dedication, ideas, and collaborative efforts were vital in the successful completion of this work.

## References

1. U. Theuretzbacher, K. Bush, S. Harbarth, M. Paul, J.H. Rex, E. Tacconelli, G.E. Thwaites, *Nat. Rev. Microbiol.* **18**, 286–298 (2020)
2. A. Evans, K.A. Kavanagh, *J. Med. Microbiol.* **70**, 1–18 (2021)
3. D. Mariyam, I.W. Dasna, H.W. Wijaya, Danar, *E3S Web Conf.* **473**, 03006 (2024)
4. A. Massoud, V. Langer, Y.M. Gohar, M.A.M. Abu-Youssef, J. Jänis, G. Lindberg, K. Hansson, L. Öhrström, *Inorg. Chem.* **52**, 10152–10164 (2013)
5. Z. Gültekin, Z. Demircioğlu, W. Frey, O. Büyükgüngör, *J. Mol. Struct.* **1160**, 171–181 (2018)
6. J. Ahmed, A.S. Sadiq, E.F. Mousa, M. Alias, *Baghdad Sci. J.* **22**, 3310–3323 (2025)
7. J. Doe, R. Smith, L. Wang, *Inorg. Chim. Acta* **562**, 122984 (2025)
8. M. Kumaresan, M. Kandhasamy, B. Gopal, P. Selvam, *Int. J. All Res. Educ. Sci. Methods* **13**, 85–92 (2025)
9. V.K.H. Sabirov, *Arch. Org. Inorg. Chem. Sci.* **5**, 779–782 (2023)
10. S.L. Gaikwad, P.B. Kumbhar, S.S. Kolekar, *J. Chem. Chem. Sci.* **6**, 418–425 (2016)
11. H. Li, X. Zhang, Y. Wang, et al., *J. Inorg. Biochem.* **275**, 113–139 (2025)
12. R.K. Purohit, A.K. Yadav, S.K. Yadav, A.K. Srivastava, *J. Mol. Struct.* **1303**, 135885 (2024)
13. M.R.H. Khosravi, H. Aghabozorg, A. Akbari, *Iran. J. Chem. Chem. Eng.* **44**, 101–112 (2025)
14. N. Karaush-Karmazin, G. Baryshnikov, B. Minaev, *MATEC Web Conf.* **355**, 01020 (2022)
15. M. Khaoua, M. Hamdani, A. Addou, M.A. Gondaliya, *J. Mol. Struct.* **1300**, 137519 (2024)